



SHORT TAKE

Monitoring of cellular senescence by DNA-methylation at specific CpG sites

Carmen M. Koch,¹ Sylvia Joussen,¹ Anne Schellenberg,¹ Qiong Lin,^{1,2} Martin Zenke^{1,2} and Wolfgang Wagner¹

¹Helmholtz-Institute for Biomedical Engineering, Stem Cell Biology and Cellular Engineering, and ²Department of Cell Biology, Institute for Biomedical Engineering, RWTH Aachen University Medical School, Aachen, Germany

Summary

Replicative senescence has fundamental implications on cell morphology, proliferation, and differentiation potential. Here, we describe a simple method to track long-term culture based on continuous DNA-methylation changes at six specific CpG sites. This epigenetic senescence signature can be used as biomarker for various cell types to predict the state of cellular senescence with regard to the number of passages, population doublings, or days of *in vitro* culture.

Key words: cellular senescence; epigenetic; DNA-methylation; mesenchymal stem cells; fibroblast.

Cellular senescence in the course of culture expansion has functional relevance: The proliferation rate and *in vitro* differentiation potential of various cell types such as mesenchymal stem cells (MSC) declines with higher passages. Furthermore, cells may acquire genetic aberrations (Meza-Zepeda *et al.*, 2008), and there is evidence for epigenetic modifications upon long-term culture (Bork *et al.*, 2010). Therefore, replicative senescence needs to be considered for quality control of cell preparations—especially in cellular therapy (Tarte *et al.*, 2010).

Commonly used parameters for cellular senescence are (i) passage number, (ii) cumulative population doublings (cPD), and (iii) the time of *in vitro* culture. These parameters need to be carefully documented throughout culture expansion—otherwise, it was so far impossible to retrospectively determine the state of senescence. Expression of senescence-associated beta galactosidase (SA-b-gal) can discern cells at the senescent stage but hardly provides a quantitative measure throughout culture expansion (Dimri *et al.*, 1995). Cellular senescence is associated with a loss of telomere integrity. However, telomere length and telomerase expression vary in different cell types and have not proven as reliable quantitative measure for replicative senescence (Prowse & Greider, 1995). Long-term culture was also associated with highly consistent gene expression changes but this method requires comparative samples of early passage and differential gene expression did not facilitate absolute quantification of cellular senescence (Schallmoser *et al.*, 2010). Recently, it has been demonstrated that long-term culture is associated with specific epigenetic modifications in DNA-methylation profiles (Bork *et al.*, 2010; Noer *et al.*, 2007; Schellenberg *et al.*, 2011; Koch *et al.*, 2011).

Therefore, we hypothesized that methylation at specific cytosine residues might provide an epigenetic signature to track the state of cellular senescence.

We have used various human cell preparations to identify a generally applicable senescence signature: Fibroblasts from different dermal regions, MSC from bone marrow (BM; iliac crest or caput femoris) or from adipose tissue (AT); culture medium was supplemented with either fetal calf serum (FCS; 2% or 10%) or human platelet lysate. Long-term growth curves demonstrated that the maximal number of cPD depends on cell type, tissue of origin, and culture medium (Fig. 1A). Senescent cells acquired typical morphological changes, stained positive for SA-b gal, displayed more lysosomes and MSC lost the capability of adipogenic and osteogenic differentiation (Fig. S1).

DNA-methylation profiles of 51 samples at different passages were analyzed with Illumina Bead Chip technology that represents 27,578 CpG sites (Table S1). Unsupervised principal components analysis (PCA) of quantil normalized raw-data demonstrated that cells from the same tissues are closely related. The second component of this analysis clearly separated samples of early and late passages. Interestingly, even the distance corresponded to the number of passages between early and late passage (Fig. 1B). This indicates that long-term culture-associated epigenetic modifications are highly reproducible and continuously acquired during expansion.

Pavlidis Template Matching (PTM) was used to identify those CpG sites with either linear increase or decrease in the methylation level according to (i) passage number, (ii) cPD, or (iii) days of *in vitro* culture. This method revealed CpG sites that become continuously hyper- or hypo-methylated in long-term culture ($P < 10^{-11}$; Fig. 1C–E). To compile a simple biomarker panel based on senescence-associated DNA-methylation changes, we have restricted further analysis to the six best suited CpG sites (Fig. 2A). These CpG sites gave the most significant results in PTM analysis and DNA-methylation levels varied more than 40% between early and late passages. Hyper-methylated CpG sites were associated with the genes glutamate receptor metabotropic 7 (GRM7) and calcium-sensing receptor (CASR); hypo-methylated CpG sites corresponded to PRAME family member 2 (PRAMEF2), selectin P (SELP), caspase 14 (CASP14), and keratin-associated protein 13-3 (KRTAP13-3). It has to be noted that these CpG sites were chosen without respect to the functional relevance of corresponding genes but only by their predictive value as epigenetic biomarker. In fact, these genes were hardly expressed in any of the cell preparations as determined by quantitative RT-PCR (data not shown). Methylation level of the six CpG sites was plotted against the number of passages (Fig. 2B), cPD or days in culture (Fig. S2). These data were used for linear regression analysis for each of the six CpG sites. Slopes and y-axis intercepts were then combined for simple models that enable predictions based on the beta-values of the six specific CpG sites. Furthermore, we compiled an online calculator that is based on these linear regressions to further simplify application of the method (<http://www.molcell.rwth-aachen.de/dms/>).

We tested the senescence signature with an independent set of 22 fibroblast and MSC preparations at different passages (Table S2,

Correspondence

Wolfgang Wagner, Helmholtz-Institute for Biomedical Engineering, Aachen University Medical School, Pauwelsstrasse 20, 52074 Aachen, Germany.
Tel.: +49 241 8088611; e-mail: wwagner@ukaachen.de

Accepted for publication 2 December 2011

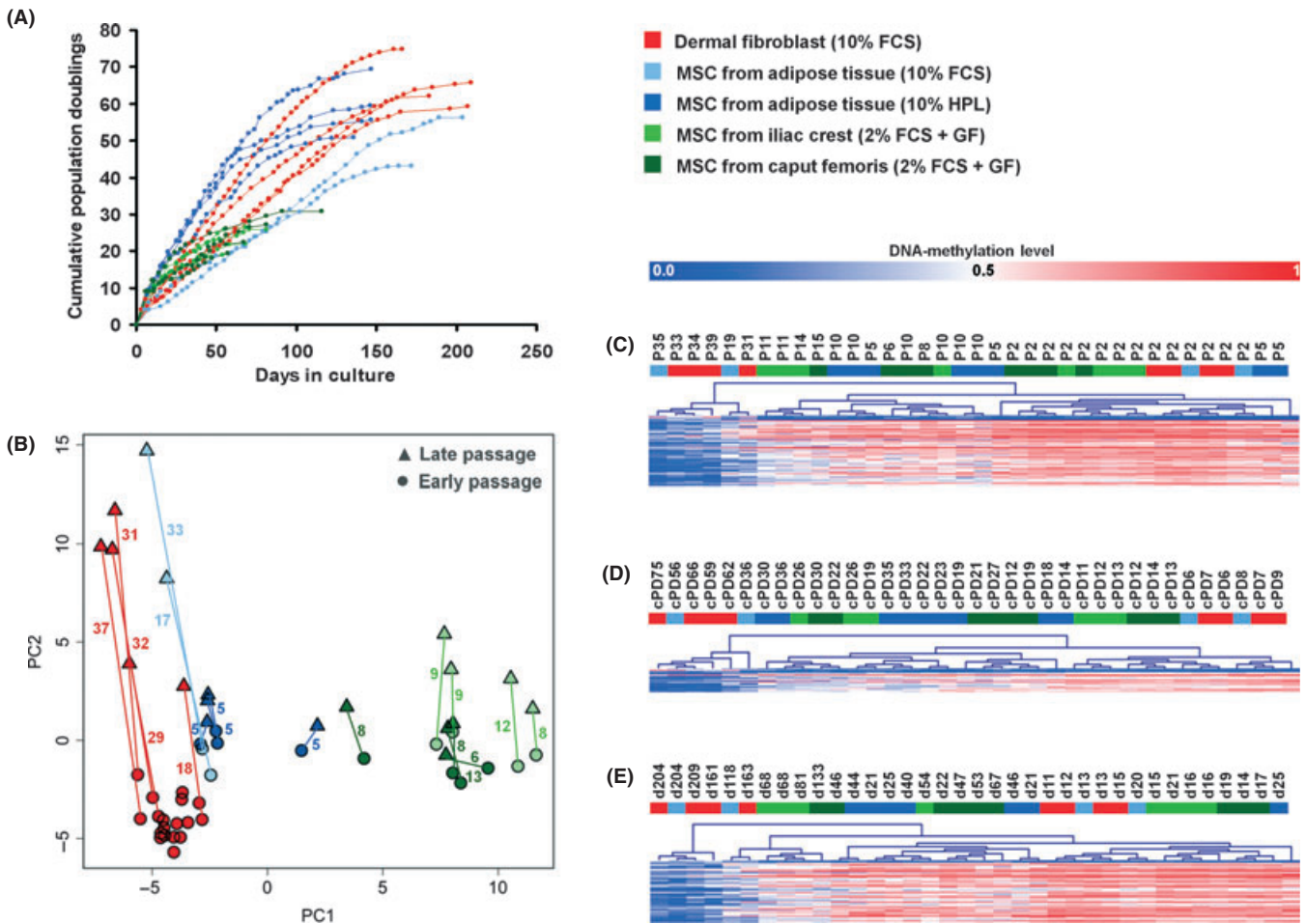


Fig. 1 Culture expansion induces DNA-methylation changes that correlate with passage numbers. (A) Long-term growth curves of dermal fibroblasts and mesenchymal stem cells, which were expanded with fetal calf serum or human platelet lysate with or without additional growth factors (GF). (B) Principal components analysis of quantil normalized DNA-methylation profiles. Corresponding samples of early and later passage are connected and the difference in passage number is indicated. (C–E) Pavlidis Template Matching identifies CpG sites with DNA-methylation level changes according to passage numbers (C; 4 CpGs hyper- and 56 CpGs hypo-methylated), cumulative population doublings (D; cPD; 3 CpGs hyper- and 17 CpGs hypo-methylated) or days of *in vitro* culture (E; 2 CpGs hyper- and 51 CpGs hypo-methylated).

Fig. S3A). In these samples, DNA-methylation level was only analyzed at the six CpG sites by pyrosequencing after bisulfite conversion. Percentages of DNA-methylation were inserted into the linear regression models for passage numbers derived from the training set of Illumina Bead Chip data. For each CpG site, the predictions correlated with the real passage numbers (Fig. S3B). Combination of the six CpG sites enabled reliable estimations of passage numbers in fibroblasts and MSC ($R^2 = 0.90$; Fig. 2C). The average difference between real and predicted passage number was three passages (with a standard deviation of four). In analogy, cPD and days in culture could be estimated by using the corresponding linear regression analyses (Fig. S3C,D). Thus, the DNA-methylation level at the six specific CpG sites can be used to monitor the state of cellular senescence of independent fibroblast and MSC samples.

Subsequently, we tested whether the epigenetic senescence signature is also applicable for very different cell types and tissues. Therefore, we have retrieved datasets with the same Illumina Bead Chip platform from public data repositories. Most of these provide little information on passage numbers. Thus, we have considered data

from either freshly isolated cells or from established cell lines. Predictions of cellular senescence were solely based on the six beta-values as described previously (Figs 2D and S4). Despite the wide range of cell types, our method could clearly separate primary cells and cultured cell lines. Notably, our method did not detect cellular senescence in datasets of ESC and iPS (Nishino *et al.*, 2011)–which do not undergo senescence in long-term culture. Thus, the state of senescence can be reversed upon reprogramming.

Long-term culture has tremendous impact on proliferation, cellular morphology, differentiation potential, and immune modulatory function. This necessitates the establishment of reliable biomarkers for cellular senescence, which are universally applicable. Our epigenetic senescence signature meets these requirements and can be used for quality control of therapeutic cell preparations. Further research will demonstrate how the predictions of passage number are affected by seeding density. The method might even be used to detect cross-contaminations of cell lines or mixing up of samples. DNA is relatively stable and can easily be shipped for cost-effective analysis by pyrosequencing. The continuous changes in DNA-methylation at

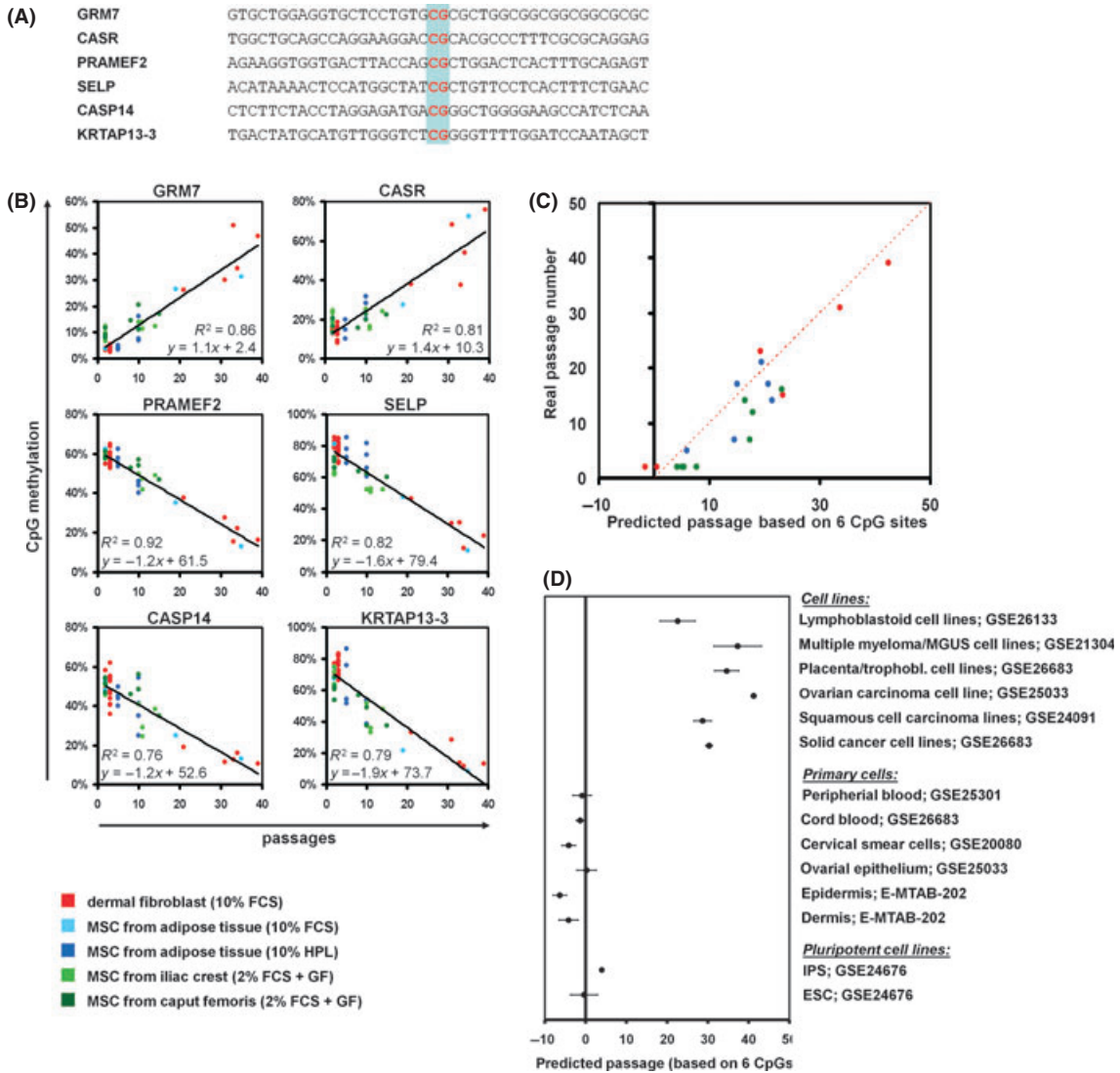


Fig. 2 Six CpG sites reflect the number of passages. (A) Genomic sequences of six CpG sites, which were used for the epigenetic senescence signature. (B) Methylation level of the CpG sites were plotted against the passage numbers for linear regression analysis. (C) Independent cell preparations were used for validation of the senescence signature by pyrosequencing of the six CpG sites. The beta-values were used for the above-mentioned linear regression models. (D) DNA-methylation datasets were retrieved from public data repositories. DNA-methylation level at the six CpG sites can clearly separate freshly isolated cells and culture expanded cell lines.

specific CpG sites facilitate reliable predictions of the state of cellular senescence.

Acknowledgments

We thank Matthias Schick (DKFZ, Heidelberg, Germany) for hybridization and preliminary analysis of DNA-methylation data. This work was supported by the excellence initiative of the German federal and state governments within the START-Program of the Faculty of Medicine, RWTH Aachen (W.W.), by the Stem Cell Network North Rhine Westphalia (W.W.) and by the Else-Kröner Fresenius Stiftung (W.W. and C.K.).

References

Bork S, Pfister S, Witt H, Horn P, Korn B, Ho AD, Wagner W (2010) DNA methylation pattern changes upon long-term culture and aging of human mesenchymal stromal cells. *Aging Cell* **9**, 54–63.

Dimri GP, Lee X, Basile G, Acosta M, Scott G, Roskelley C, Medrano EE, Linskens M, Rubelj I, Pereira-Smith O (1995) A biomarker that identifies senescent human cells in culture and in aging skin *in vivo*. *Proc. Natl Acad. Sci. U S A* **92**, 9363–9367.

Koch C, Suschek CV, Lin Q, Bork S, Goergens M, Jousen S, Pallua N, Ho AD, Zenke M, Wagner W (2011) Specific age-associated DNA methylation changes in human dermal fibroblasts. *PLoS One* **6**, e16679.

Meza-Zepeda LA, Noer A, Dahl JA, Micci F, Myklebost O, Collas P (2008) High-resolution analysis of genetic stability of human adipose tissue stem cells cultured to senescence. *J. Cell Mol. Med.* **12**, 553–563.

Nishino K, Toyoda M, Yamazaki-Inoue M, Fukawatase Y, Chikazawa E, Sakaguchi H, Akutsu H, Umezawa A (2011) DNA methylation dynamics in human induced pluripotent stem cells over time. *PLoS Genet.* **7**, e1002085.

Noer A, Boquest AC, Collas P (2007) Dynamics of adipogenic promoter DNA methylation during clonal culture of human adipose stem cells to senescence. *BMC Cell Biol.* **8**, 18.

Prowse KR, Greider CW (1995) Developmental and tissue-specific regulation of mouse telomerase and telomere length. *Proc. Natl Acad. Sci. U S A* **92**, 4818–4822.

Schallmoser K, Bartmann C, Rohde E, Bork S, Guelly C, Obenauf AC, Reinisch A, Horn P, Ho AD, Strunk D, Wagner W (2010) Replicative senescence-associated

gene expression changes in mesenchymal stromal cells are similar under different culture conditions. *Haematologica* **95**, 867–874.

Schellenberg A, Lin Q, Schueler H, Koch C, Jousseaume S, Denecke B, Walenda G, Pallua N, Suschek C, Zenke M, Wagner W (2011) Replicative senescence of mesenchymal stem cells causes DNA-methylation changes which correlate with repressive histone marks. *Aging (Albany NY)* **3**, 873–888.

Tarte K, Gaillard J, Lataillade JJ, Fouillard L, Becker M, Mossafa H, Tchirkov A, Rouard H, Henry C, Splingard M, Dulong J, Monnier D, Gourmelon P, Gorin NC, Sensebe L (2010) Clinical-grade production of human mesenchymal stromal cells: occurrence of aneuploidy without transformation. *Blood* **115**, 1549–1553.

Supporting Information

Additional supporting information may be found in the online version of this article:

Fig. S1 Characterization of culture-expanded stromal cells.

Fig. S2 Methylation changes with regard to cumulative population doublings (cPD) and days in culture.

Fig. S3 Cell preparations for validation by pyrosequencing.

Fig. S4 DNA-methylation level at the six CpG sites in different tissues and cell lines.

Table S1 Cell preparations used for DNA-methylation profiling.

Table S2 Cell preparations used for validation by pyrosequencing.

As a service to our authors and readers, this journal provides supporting information supplied by the authors. Such materials are peer-reviewed and may be re-organized for online delivery, but are not copy-edited or typeset. Technical support issues arising from supporting information (other than missing files) should be addressed to the authors.